Anal Bioanal Chem (2013) 405:9843–9848
DOI 10.1007/s00216-013-7426-8

RESEARCH PAPER

Comparative direct infusion ion mobility mass spectrometry profiling of *Thermus thermophilus* wild-type and mutant Δ*cruC* carotenoid extracts

Timo D. Stark · Angel Angelov · Mathias Hofmann · Wolfgang Liebl · Thomas Hofmann

Received: 26 August 2013 / Revised: 4 October 2013 / Accepted: 7 October 2013 / Published online: 10 November 2013

Abstract The major carotenoid species isolated from the thermophilic bacterium *Thermus thermophilus* HB27 have been identified as zeaxanthin–glucoside–fatty acid esters (thermozeaxanthins and thermobiszeaxanthins). Most of the genes of the proposed *T. thermophilus* carotenoid pathway could be found in the genome, but there is less clarity about the genes which encode the enzymes performing the final carotenoid glycosylation and acylation steps. To get a further insight into the biosynthesis of thermo(bis)zeaxanthins in *T. thermophilus*, we deleted the megaplasmid open reading frame TT_P0062 (termed *cruC*) by both exchanging it with a kanamycin resistance cassette (Δ*cruC*:kat) and by generating a markerless gene deletion strain (Δ*cruC*). A fast and efficient electrospray ionization–ion mobility–time-of-flight mass spectrometry method via direct infusion was developed to compare the carotenoid profiles of wild type and mutant *T. thermophilus* cell culture extracts. These comparisons revealed significant alterations in the carotenoid composition of the Δ*cruC* mutant, which was found to accumulate zeaxanthin. This is the first experimental evidence that the ORF encodes the glycosyltransferase enzyme necessary for the glycosylation of zeaxanthin in the final modification steps of the thermozeaxanthin biosynthesis in *T. thermophilus* HB27. Also, the proposed method for direct determination of carotenoid amounts and species in crude acetone extracts represents an improvement over existing methods in terms of speed and sensitivity and may be applicable in high-throughput analyses of other terpenoids as well as other important bacterial metabolites like fatty acids and their derivatives.

Keywords ESI–IM–TOFMS · Thermozeaxanthins · Ion mobility separation · *Thermus thermophilus* · Carotenoids

Timo D. Stark and Angel Angelov contributed equally to this work.

Electronic supplementary material The online version of this article (doi:10.1007/s00216-013-7426-8) contains supplementary material, which is available to authorized users.

T. D. Stark (✉) · T. Hofmann
Food Chemistry and Molecular Sensory Science,
Technische Universität München,
Lise-Meitner Str. 34, 85354 Freising, Germany
e-mail: timo.stark@tum.de

A. Angelov · W. Liebl
Microbiology, Technische Universität München,
Emil-Ramann-Str. 4, 85354 Freising, Germany

M. Hofmann
Waters, Helfmann-Park 10, 65760 Eschborn, Germany

Introduction

In photosynthetic organisms, carotenoids fulfill multiple physiological roles such as accessory pigments in light-harvesting complexes and protectors against photooxidative damage. In contrast, the role of carotenoid compounds in non-phototrophic organisms is less clear. Many strains of the thermophilic bacterium *Thermus* are known to produce carotenoids in a light-dependent manner [1]. The major carotenoid species isolated from *T. thermophilus* HB27 are thermozeaxanthins (Fig. 1, **4**–**7**) and thermobiszeaxanthins [2, 3]. These molecules have been identified as zeaxanthin-glucoside-fatty acid esters, carrying acyl moieties of varying length (C11 to C17). While glucosylation is a common modification found in carotenoids of various origins, the presence of glycoside-fatty acid esters is more seldom. Interestingly, fatty acid-glycoside esters of carotenoids are found in other phylogenetically distant, thermophilic and halophilic organisms, for example *Thermomicrobium roseum* [4] and *Salinibacter ruber* [5]. Although the physiological impact of such carotenoid modifications is not clear, it is assumed that they affect membrane rigidity in response to

stress conditions. In *T. thermophilus* the highly hydrophobic zeaxanthin-glucoside-fatty acid esters may stabilize the membrane at high temperatures via positioning the zeaxanthin moiety in the lipid bilayer while the glucose moiety resides at the surface of the membrane, and the branched fatty acid moiety curls back into the lipid bilayer [2].

In the genome of *Thermus thermophilus* HB27, the genes encoding the carotenoid biosynthesis pathway are distributed among both parts of the genome, i.e. the chromosome and the megaplasmid pTT27 [1]. The genes for the methyl-D-erythritol-4-phosphate (MEP) pathway, leading to the carotenoid precursors isopentenyl pyrophosphate (IPP) and dimethylallyl pyrophosphate (DMAPP) are located on the chromosome, while the genes for the terminal carotenoid pathway enzymes are found on the megaplasmid pTT27. Based on sequence similarity to known and well-conserved carotenoid biosynthesis proteins and gene expression studies, almost all of the genes of the proposed *T. thermophilus* carotenoid pathway could be found in the genome [6–8]. However, there is less clarity about the genes which encode the enzymes performing the final carotenoid glycosylation and acylation steps.

Based on the genomic context of the *T. thermophilus* HB27 open reading frame (ORF) TT_P0062 and on the presence of a glycosyltransferase domain in the predicted protein (Glycosyltransferase like family 2, Pfam), we hypothesized that this ORF encodes the enzyme necessary for the glycosylation of zeaxanthin (**3**, Fig. 1) in the final modification steps of the thermozeaxanthin synthesis in *T. thermophilus* HB27. To test this hypothesis, we deleted the TT_P0062 ORF (termed *cruC*) by both exchanging it with a kanamycin resistance cassette (Δ*cruC:kat*) and by generating a markerless gene deletion strain (Δ*cruC*). The successful allelic exchange at the *cruC* locus in both strains was confirmed by PCR and Southern blot (Fig. 2).

The electrospray ionization (ESI)–time-of-flight mass spectrometry (TOFMS) approach in combination with ultra-performance liquid chromatography (UPLC) was recently successfully used for high-throughput demand and enabled the rapid detection and quantitation of bioactives [9, 10] and urinary dietary biomarkers for coffee consumption [11]. Generally, ion mobility (IM) separation enables a fast alternative separation approach without time-consuming stationary phase, buffer and gradient testing in liquid chromatography of these extremely hydrophobic carotenoid derivatives. Metabolite and secondary metabolite discovery was already successfully applied using IM–mass spectrometry (MS) [12, 13].

To prove the hypothesis that the ORF encodes the enzyme necessary for the glycosylation of zeaxanthin in the final modification steps of the thermozeaxanthin synthesis in *T. thermophilus* HB27, we compared the carotenoid profiles of wild-type *T. thermophilus* HB27 and of the Δ*cruC*:kat mutant by means of direct infusion and IM–TOFMS.

Chemicals

Chemicals and reagents

The following compounds were obtained commercially: β-carotene and zeaxanthin (**1**, **3**, Fig. 1) (Sigma-Aldrich, Steinheim, Germany); solvents (acetone, methyl *tert*-butylether and isopropanol) used were of HPLC-grade (Merck, Darmstadt, Germany).

Bacterial strains and growth conditions

Escherichia coli XL1-Blue (Agilent Technologies, Santa Clara, USA) was used as a host for DNA manipulations and was grown in LB medium (10 g/L tryptone, 5 g/L yeast extract, 5 g/L NaCl) at 37 °C. *T. thermophilus* HB27 wild type (DSM 7039) and derivative strains were grown at 70 °C with vigorous shaking in TB medium. TB medium had a pH of 7.5 and contained per liter 8 g trypticase peptone, 4 g yeast extract, and 3 g NaCl, and was prepared with a high-carbonate mineral water (Purania, DRINKPOOL GmbH, Germany). In order to obtain large amounts of the carotenoid species for IM–TOFMS measurements, 1-L cultures of *T. thermophilus* wild-type and Δ*cruC*:kat were grown for 12 h at 60 °C in Erlenmeyer flasks (5 L) with vigorous shaking and under constant exposure to white light, supplied by white light fluorescent lamps.

Inactivation of the *cruC* gene

Initially, the ORF TT_P0062 was inactivated by replacement with a kanamycin resistance marker cassette (*kat*) by homologous recombination. The allelic replacement vector pUC-ΔcruC was obtained by blunt-end cloning of a 3,930 bp region containing 1,269 bp of upstream and 1,639 bp of downstream sequences of the TT_P0062 ORF in the SmaI site of the pUC18 vector. This construct was subjected to site-directed mutagenesis with oligonucleotides 62 m1 and 62 m2 which introduce *Bgl*II sites at positions 11 and 1,016 relative to the *cruC* start codon (primer sequences are listed in Electronic Supplementary Material (ESM), Table S1). *Bgl*II restriction followed by re-ligation gave pUC-ΔcruC in which the whole coding sequence of the *cruC* gene was deleted (amino acid positions 4 to 339). The *Bam*HI fragment containing the *kat* cassette was obtained from the vector pMK18 [14] and was cloned in the *BglII* site of pUC-ΔcruC, giving pUC-ΔcruC:*kat*.

An unmarked *cruC* deletion strain (Δ*cruC*) devoid of any foreign DNA fragments was created by transforming *T. thermophilus* HB27 with the pUC-Δ*cruC* vector, followed by a PCR-based screen of several hundred colonies with primers d62-F and d62-R to identify the knockout allele in the genome.

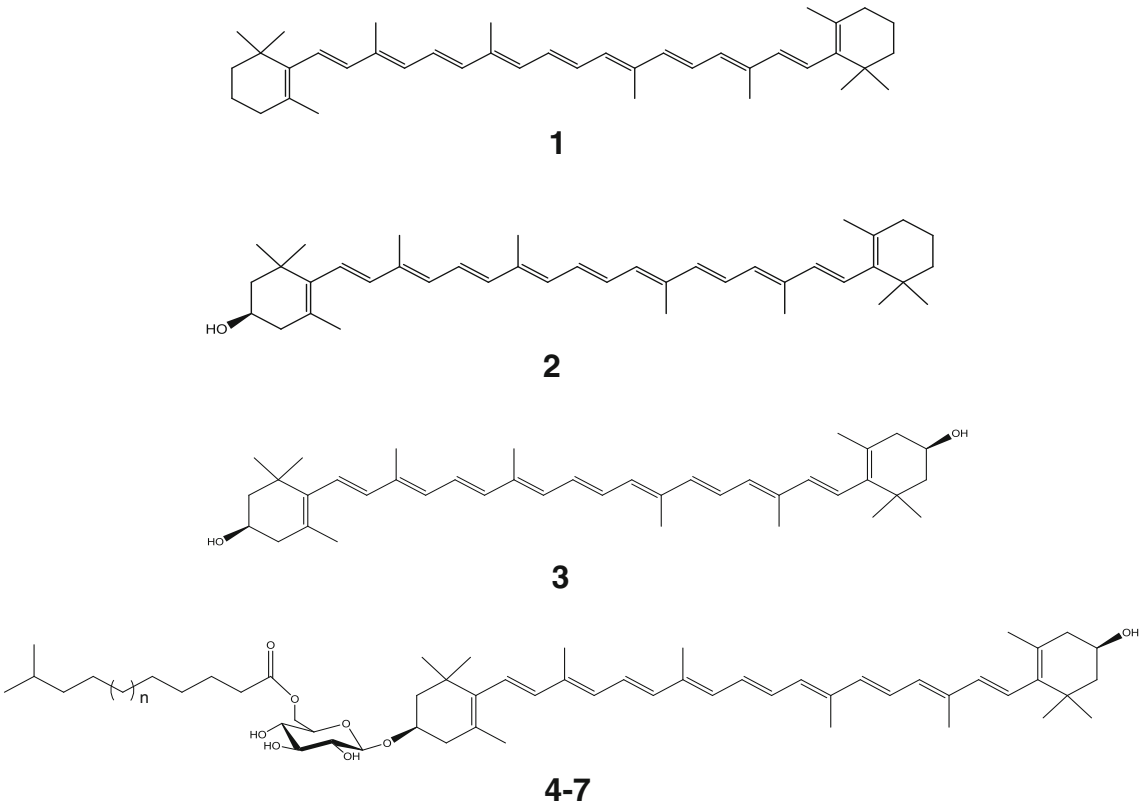

Fig. 1 Chemical structures of β-carotene (**1**), β-cryptoxanthin (**2**), zeaxanthin (**3**), thermozeaxanthin-11 ($n=1$; **4**), thermozeaxanthin-13 ($n=2$; **5**) thermozeaxanthin-15 ($n=3$; **6**), thermozeaxanthin-17 ($n=4$; **7**)

Carotenoid extraction

T. thermophilus cells were collected by centrifugation (20 min at 13,000*g*), extracted with acetone, and the solvent was removed under reduced pressure (40 °C), redissolved in a mixture of methyl *tert*-butylether and isopropanol (15 mL, 1/14, *v*/*v*), and after membrane filtration (0.45 μm) directly used for ESI–IM–TOFMS.

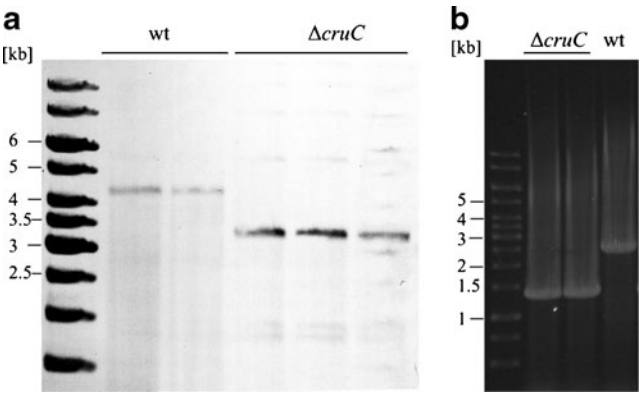

Fig. 2 Southern blot (**A**) and PCR (**B**) analysis of the genotype of the *T. thermophilus* HB27 strain Δ*cruC*. For the Southern blot, genomic DNA isolated from colonies of the wild-type and the Δ*cruC* strain was digested with BamHI and hybridized with a biotin-labeled probe. The in silico predicted size is 4,327 bp for the wt and 3,295 bp for the Δ*cruC* strain. PCR was performed with genomic DNA isolated from the respective strains with primers d62f and d62r (primer sequences are listed in Table S1, Electronic Supplementary Material). Predicted sizes of the PCR products are 2,309 bp for the wt and 1,303 bp for the Δ*cruC* strain

Ion mobility time-of-flight mass spectrometry

Mass spectrometry and ion mobility measurements were performed using a Synapt G2 HDMS mass spectrometer (Waters, Manchester, UK). Samples were directly infused for 1 min via the fluidics system (20 μL/min). Measurements were performed using positive ESI and the resolution mode consisting of the following parameters: capillary voltage + 3.0 kV, sampling cone 30 V, extraction cone 4.0 V, source temperature 150 °C, desolvation temperature 250 °C, cone gas 30 L/h, desolvation gas 550 L/h, helium cell pressure 1.4 mbar, ion mobility cell pressure 3.45 mbar of nitrogen, cooling gas flow 10.00 mL/min, trap gas flow 2.00 mL/min, helium cell gas flow 180.00 mL/min, IM gas flow 90.00 mL/min, IM wave velocity 350 m/s and IM wave height 40 V. For IM, a mass range from m/z 50–1,200 with scan time for the MS method (continuum) was set to 2 s. Data processing was performed by using HDMS compare software 1.0 and MassLynx 4.1 SCN 779 (Waters) and the elemental composition tool for determining the elemental composition.

All data were lock mass corrected on the pentapeptide leucine enkephaline (Tyr-Gly-Gly-Phe-Leu, *m/z* 556.2771, $[M+H]^+$) in a solution (2 ng/μL) of acetonitrile/0.1 % formic acid (1/1, *v/v*). Scan time for the lock mass was set to 1 s, an interval of 10 s and three scans to average with a mass window of ±0.5 Da. Calibration of the Synapt G2 in the range from *m/z* 50–1,200 was performed using a solution of sodium formate (5 mmol/L) in 2-propanol/water (9/1, *v/v*).

β-carotene, **1** (Fig. 1), *m/z* 536.4371$^{\bullet+}$ (calcd for $[C_{40}H_{56}]^+$ 536.4382, Δ—2.1 ppm); β-cryptoxanthin, **2** (Fig. 1), *m/z* 552.4321$^{\bullet+}$ (calcd for $[C_{40}H_{56}O]^+$ 552.4331, Δ—1.8 ppm); zeaxanthin, **3** (Fig. 1), *m/z* 568.4270$^{\bullet+}$ (calcd for $[C_{40}H_{56}O_2]^+$ 568.4280, Δ—1.8 ppm), zeaxanthin-Na, *m/z* 591.4160$^+$ (calcd for $[C_{40}H_{56}O_2Na]^+$ 591.4178, Δ—3.0 ppm), zeaxanthin-K, *m/z* 607.3965$^+$ (calcd for $[C_{40}H_{56}O_2K]^+$ 607.3917, Δ+7.9 ppm); Z1-11 thermozeaxanthin-11, **4** (Fig. 1), *m/z* 898.6294$^{\bullet+}$ (calcd for $[C_{57}H_{86}O_8]^+$ 898.6223, Δ—3.0 ppm), *m/z* 921.6203$^+$ (calcd for $[C_{57}H_{86}O_8Na]^+$ 921.6220, Δ—1.8 ppm), *m/z* 937.5953$^+$ (calcd for $[C_{57}H_{86}O_8K]^+$ 937.5960, Δ—0.7 ppm); Z1-13 thermozeaxanthin-13, **5** (Fig. 1), *m/z* 926.6583$^{\bullet+}$ (calcd for $[C_{59}H_{90}O_8]^+$ 926.6636, Δ—5.3 ppm), *m/z* 949.6511$^+$ (calcd for $[C_{59}H_{90}O_8Na]^+$ 949.6533, Δ—2.3 ppm), *m/z* 965.6279$^+$ (calcd for $[C_{59}H_{90}O_8K]^+$ 965.6273, Δ+0.6 ppm); Z1-15 thermozeaxanthin-15, **6** (Fig. 1), *m/z* 954.6924$^{\bullet+}$ (calcd for $[C_{61}H_{94}O_8]^+$ 954.6949, Δ—2.5 ppm), *m/z* 977.6827$^{\bullet+}$ (calcd for $[C_{61}H_{94}O_8Na]^+$ 977.6846, Δ—1.9 ppm), *m/z* 993.6609$^+$ (calcd for $[C_{61}H_{94}O_8K]^+$ 993.6586, Δ+2.3 ppm); Z1-17 thermozeaxanthin-17, **7** (Fig. 1), *m/z* 1005.7111$^+$ (calcd for $[C_{63}H_{98}O_8Na]^+$ 1005.7159, Δ—4.8 ppm), *m/z* 1021.6889$^+$ (calcd for $[C_{63}H_{98}O_8K]^+$ 1021.6899, Δ—1.0 ppm). MS/MS experiments with thermozeaxanthins showed fingerprint fragment ions which were identified with a mass accuracy of 2 ppm as the zeaxanthin aglycon as well as zeaxanthin-glucoside. Data from HDMS compare software was exported into Microsoft Excel 2010 for further data processing, giving drift time accurate mass and area of every *m/z*.

Results and discussion

Based on its genomic context and on the presence of a glycosyltransferase domain (glycosyltransferase like family 2, according to Pfam classification) in the predicted protein the *T. thermophilus* HB27 ORF TT_P0062 was identified as a candidate ORF that could encode the enzyme necessary for the glycosylation of zeaxanthin in the final modification steps of the thermozeaxanthin synthesis in *T. thermophilus* HB27. To test this hypothesis, we deleted the TT_P0062 ORF (termed *cruC*) by both exchanging it with a kanamycin resistance cassette (*ΔcruC:kat*) and by generating a markerless gene deletion strain (*ΔcruC*). The successful allelic exchange at the *cruC* locus in both strains was confirmed by PCR and Southern blot (Fig. 2). The *cruC* deletion strains were undistinguishable from the wild type both in their growth rate at the optimal growth temperature of *T. thermophilus* and in the yellow color of the bacterial colonies which they developed after exposure to white light. Also, the UV–Vis absorbance spectra of acetone extracts from both strains showed only a minor difference, representing a small hypsochromic shift of 2 nm in the Δ*cruC:kat* strain (ESM, Fig S1). In order to investigate the changes in carotenoid amounts and composition resulting from the inactivation of the *cruC* gene, acetone extracts from both strains were subjected to direct ESI^+–IM–TOFMS.

The cells of both strains were collected by centrifugation, extracted with acetone, the solvent evaporated, redissolved in a mixture of methyl *tert*-butylether and isopropanol, and after membrane filtration directly used for ESI^+–IM–TOFMS. In Fig. 3, the drift time (microseconds) vs. *m/z* in a range from 50 to 1,200 of the direct infusion of the *T. thermophilus* mutant *ΔcruC:kat* is given. β-Carotene (**1**) and zeaxanthin (**3**) were identified as radical cations ($M^{\bullet+}$) in the extract by co-separation and accurate mass via direct infusion of these reference compounds. The existence of radical cations ($M^{\bullet+}$) of these compounds is in line with literature data [15, 16]. Also the sodium and potassium adduct of zeaxanthin were observable ($[M+Na]^+$, $[M+K]^+$) at higher drift times. β-Cryptoxanthin ($C_{40}H_{56}O$) (**2**, Fig. 1), as the decisive intermediate of the carotenoid biosynthesis from β-carotene (**1**, $C_{40}H_{56}$) to zeaxanthin (**3**, $C_{40}H_{56}O_2$), was identified on basis of accurate mass and drift time. The drift time of all three carotenoids was in a very similar range from 4.07–4.14 ms. The thermozeaxanthins Z1-11 to Z1-17 (**4**–**7**), as the major expected metabolites for a working carotenoid biosynthesis were hardly detectable in the expected mass range from *m/z* 900–1,100. In contrast, infusion of the *T. thermophilus* wild-type extract (Fig. 3) revealed several signals for thermozeaxanthins (**4**–**7**) in the expected mass range from *m/z* 900–1,100. The drift time for all relevant signals in this range was between 6.65 and 7.03 ms, and, therefore significantly increased in comparison to the compounds **1**–**3**. The differences between both samples are presented in Fig. 3, which compares both samples via a difference plot. In this plot, the mass range *m/z* 530–620 is stronger expressed in the mutant sample, whereas the mass range *m/z* 900–1,050 is stronger expressed in the wild type sample. Compounds **1**–**3** were responsible for the differences in the mass range *m/z* 530–620 which were identified in both samples as described above. Thermozeaxanthins (**4**–**7**) could be mainly detected as their sodium adducts, followed by their potassium adducts as well as traces of radical cations. In particular, the most abundant signal *m/z* 949.6511 was identified as the sodium adduct of thermozeaxanthin Z-1-13 (5) (calcd for $[C_{59}H_{90}O_8Na]^+$ 949.6533) with a difference of 2.3 ppm, followed by the sodium adduct of thermozeaxanthin Z-1-15

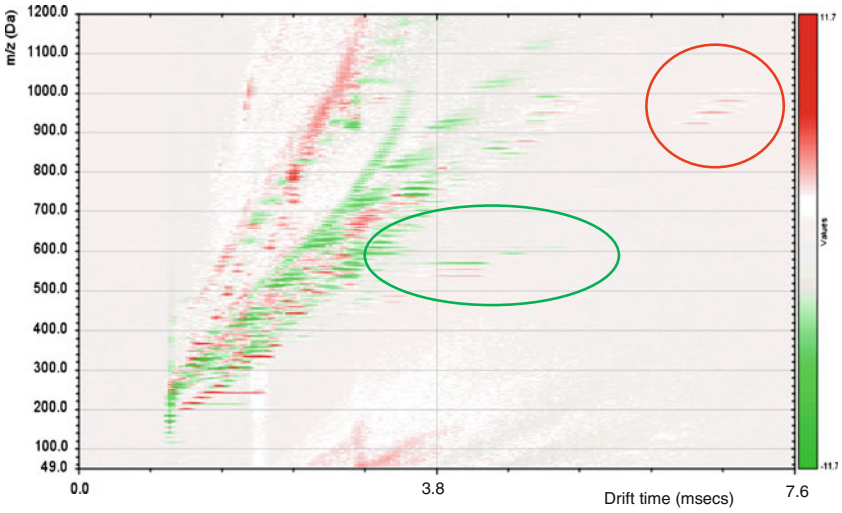

Fig. 3 Differential plot of ESI^+–IM–TOFMS separation of *T. thermophilus* HB27 wild-type (*red*) and mutant Δ*cruC*:*kat* (*green*) cell culture extract. Drift time (milliseconds) vs. *m*/*z* (50-1200)

(6) *m*/*z* 977.6827$^+$ (calcd for $[C_{61}H_{94}O_8Na]^+$ 977.6846, Δ—1.9 ppm) and the sodium adduct of thermozeaxanthin Z-1-11 (4) *m*/*z* 921.6203$^+$ (calcd for $[C_{57}H_{86}O_8Na]^+$ 921.6220, Δ—1.8 ppm) (ESM, Fig. S2A+B). The mass accuracy enabled us to determine the elemental composition of the corresponding potassium adducts as well as radical cations of compounds **4**–**7** in both samples, respectively. On the basis of the higher drift time as well as the mass accuracy, resulting in the matching elemental compositions of all adducts and occurring radical cations of each thermozeaxanthin, the thermozeaxanthins Z-1-11 to Z-1-17 (**4**–**7**) were clearly identified in both extracts.

The signal intensity for thermozeaxanthins (**4**–**7**) in both samples was quite different. While the wild-type sample showed a base peak intensity of 6.3e^4 for the potassium adduct of 5, the base peak signal intensity in the mutant sample was decreased by a factor of 58. The most abundant signal for compounds **1**–**3** in the wild-type sample is β-cryptoxanthin (**2**, ESM, Fig. S3B), whereas the dominating compound in the mutant sample is zeaxanthin (**3**, ESM Fig. S3A). In the mutant, the possible glycosylated derivatives of compounds **2**–**3**, yielding potential intermediates of the biosynthesis of thermozeaxanthins could not be detected either as radical ions or as sodium or potassium ion adducts in both samples. The observation that no non-esterified mono- and/or diglucosides were detected in extracts from wild type cells can be explained by very low amounts of these intermediates, which may be due to their rapid esterification my means of an acyl transferase, the next enzyme in the biosynthetic pathway. This is in agreement with previous reports [3].

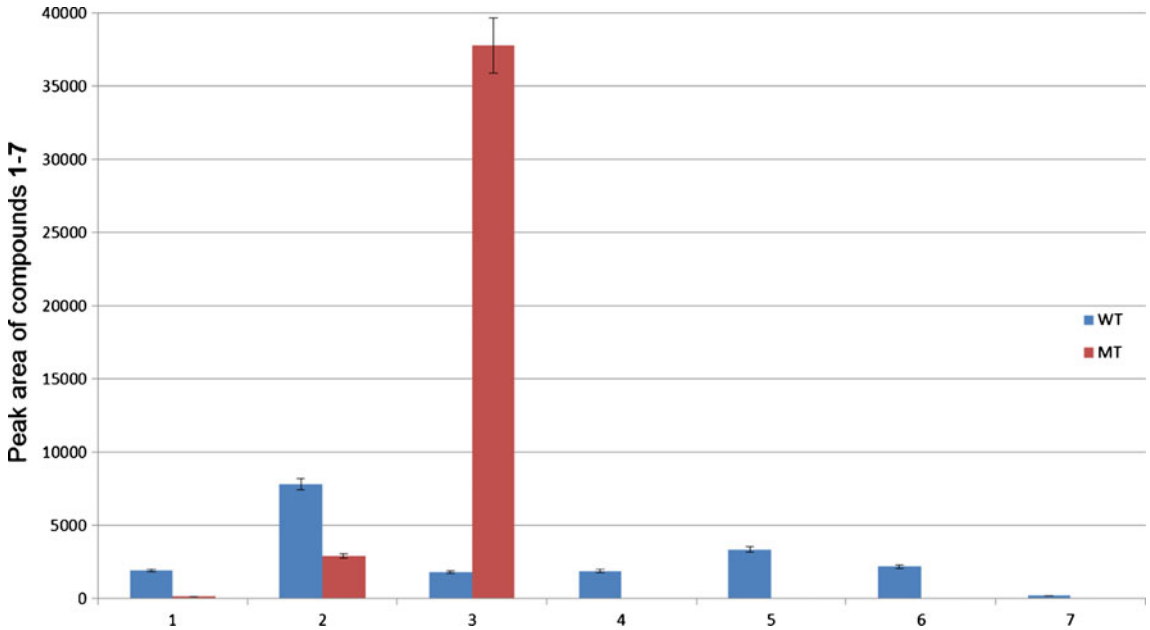

Fig. 4 Relative quantitative data of compounds **1**–**7**. WT and MT represent wild type and *ΔcruC:kat*, respectively

For a direct relative quantitative comparison of both samples, IM–TOFMS data from the HDMS compare software was exported into Microsoft Excel for further data processing, giving drift time, accurate mass and areas of every m/z. The corresponding areas for radical cations, sodium, and potassium adducts of compounds 1–7 were summed up and shown in Fig. 4. As indicated in Figs. 3 and 4 and ESM Figs. S2–S3 by differential plot or comparing signal intensities, the mutant strain was blocked in the biosynthesis of thermozeaxanthins after producing zeaxanthin (**3**), whose concentration was extremely high. Minor amounts of β-cryptoxanthin (**2**) were also detected in the mutant strain. In comparison to the mutant strain (Fig. 4), the biosynthesis of thermozeaxanthins **4**–**7** in the wild-type strain was not genetically modified, and, therefore, yielding relative low amounts of zeaxantin (**3**) and good biosynthesis rates of thermozeaxanthins **4**–**7**. These results clearly indicate that by deleting the *T. thermophilus* HB27 ORF TT_P0062 by both exchanging it with a kanamycin resistance cassette (*ΔcruC:kat*) and by generating a markerless gene deletion strain (*ΔcruC*), the glycosylation of β-cryptoxanthin and of zeaxanthin were abolished.

Conclusion

By means of direct infusion in combination with ESI–IM–TOFMS, a fast and efficient approach was developed to analyze the carotenoids of *T. thermophilus* directly in cell culture acetone extracts. By means of comparison of the carotenoid profiles of wild-type and a knockout of a hypothetical glycosyltransferase gene, significant differences in the concentrations of compounds **1**–**3** as well as the end products of biosynthesis, namely thermozeaxanthins **4**–**7**, could be disclosed. This is the first experimental evidence that the ORF TT_P0062 encodes the enzyme necessary for the glycosylation of zeaxanthin (**3**, Fig. 1) in the final modification steps of the thermo(bis)zeaxanthins biosynthesis in *T. thermophilus* HB27.

Acknowledgments We are grateful to Sofie Lösch and Beate Schumacher for technical assistance. Part of this work was supported by the Bundesministerium für Bildung, Wissenschaft, Forschung und Technologie within the framework of the GenoMik (Genomforschung an Mikroorganismen) funding measure (FKZ 0315586A).

References

1. Brock TD (1978) Springer series in microbiology. The genus *Thermus*: 72–91
2. Yokoyama A, Sandmann G, Hoshino T, Adachi K, Sakai M, Shizuri Y (1995) Tetrahedron Lett 36:4901–4904
3. Yokoyama A, Shizuri Y, Hoshino T, Sandmann G (1996) Arch Microbiol 165:342–345
4. Wu D, Raymond J, Wu M, Chatterji S, Ren Q, Graham JE, Bryant DA, Robb F, Colman A, Tallon LJ, Badger JH, Madupu R, Ward NL, Eisen JA (2009) PLoS ONE 4:e4207
5. Lutnaes BF, Oren A, Liaaen-Jensen S (2002) J Nat Prod 65:1340–1343
6. Henne A, Brüggemann H, Raasch C, Wiezer A, Hartsch T, Liesegang H, Johann A, Lienard T, Gohl O, Martinez-Arias R, Jacobi C, Starkuviene V, Schlenczeck S, Dencker S, Huber R, Klenk HP, Kramer W, Merkl R, Gottschalk G, Fritz HJ (2004) Nat Biotechnol 22:547–553
7. Tian B, Hua Y (2010) Trends Microbiol 18:512–520
8. Hoshino T, Fujii RTN (1993) Appl Environ Microbiol 59:3150–3153
9. Stark T, Marxen S, Rütschle A, Lücking G, Scherer S, Ehling-Schulz M, Hofmann T (2013) Anal Bioanal Chem 405:191–201
10. Stark T, Wollmann N, Lösch S, Hofmann T (2011) Anal Chem 83:3398–3405
11. Lang R, Wahl A, Stark T, Hofmann T (2011) Mol Nutr Food Res 55:1613–1623
12. Derewacz DK, Goodwin CR, McNees CR, McLean JA, Bachmann BO (2013) Proc Natl Acad Sci U S A 110(6):2336–2341
13. Goodwin CR, Fenn LS, Derewacz DK, Bachmann BO, McLean JA (2012) J Nat Prod 67:48–53
14. De Grado M, Castán P, Berenguer JA (1999) Plasmid 42:241–245
15. Van Breemen RB (1995) Anal Chem 67:2004–2009
16. Chu FL, Pirastru L, Popovic R, Sleno L (2011) J Agric Food Chem 59:3003–3013